Communications Research Centre

THE HIGH ARCTIC TROPOSCATTER EXPERIMENT: FINAL REPORT

by

C. Bilodeau and K.S. McCormick

anada
ommunications

Gouvernement du Canada
Ministère des Communications

Canada

THE HIGH ARCTIC TROPOSCATTER EXPERIMENT: FINAL REPORT

by

C. Bilodeau and K.S. McCormick
(Communications Technologies Research)

(Radio Networks)

COMMUNICATIONS RESEARCH CENTRE INDUSTRY AND SCIENCE
CRC REPORT NO. 94-002

Canada

April 1994
Ottawa

The High Arctic Troposcatter Experiment: Final Report

C. Bilodeau and K. S. McCormick
Industry Canada
Communications Research Centre
P. O. Box 11490, Station H
Ottawa, Canada
K2H 8S2

ABSTRACT

Experimental results of radio propagation measurements at 853 MHz are given for a 500 km troposcatter link in the Canadian High Arctic. Statistical analysis of path loss and fading measurements are presented.

The experimental data were acquired using a narrow band measurement system that was developed to permit a transmitting power of only 100 Watts while using a 4.5 metre dish at each end of the link. The system includes a digital signal processor (DSP) receiver for signal strength computation and a high stability noise source reference for amplitude calibration. The main characteristics of this system are described in this paper.

Detailed fading distributions are presented for examples of slow and fast fading periods and compared with Rayleigh distributions. An estimate of the long term median path loss is made and compared with values predicted using accepted techniques. The results are believed to be the first ever presented for a microwave troposcatter link above the 80th parallel.

RÉSUMÉ

Ce rapport présente les résultats d'une expérience de propagation radio effectuée à 853 MHz sur un trajet soumis à la diffusion troposphérique dans l'Arctique canadien. Une analyse statistique des mesures d'évanouissement et d'affaiblissement du signal est incluse.

Les données expérimentales ont été obtenues à l'aide d'un système de mesure à bande étroite, développé dans le but d'opérer avec une puissance de transmission d'à peine 100 Watts et une antenne parabolique de 4.5 mètres de diamètre à chaque extrémité de la liaison. Le système de mesure est doté d'un récepteur radio utilisant un processeur de signaux numériques pour le calcul de la puissance reçue, de même que d'une source de bruit référentielle, très stable, nécessaire à la calibration des amplitudes mesurées. Les principales caractéristiques de ce système sont décrites dans ce rapport.

Les statistiques des évanouissements sont présentées sous forme d'ogives détaillées, regroupées selon des périodes où les fluctuations observeées sont lentes ou rapides. La distribution classique de Rayleigh est utilisée pour fin de comparaison. L'affaiblissement médian à long terme du signal propagé est évalué, puis comparé aux valeurs obtenues par les techniques de prédiction conventionnelles. On pense que ces résultats sont les tout premiers à être présentés pour une liaison par ondes décimétriques et diffusion troposphérique, située au delà du quatre-vingtième parallèle.

EXECUTIVE SUMMARY

A request was formulated by DCEM-2 (see [1]) to investigate the feasibility of using a troposcatter system as an alternate for the existing microwave High Arctic Data Communication System (HADCS) between Alert and Eureka. DRDCS endorsed and sponsored a path loss study proposed by CRC to obtain system performance data since no data was available for the high arctic. Based on a review of meteorological and topographical data for the two sites [2], a site survey was conducted by representatives of CRC, DND and Harris RF Systems Division during the period 20-30 June 1988 to locate sites suitable for the study [3].

The present report summarizes the most important results of the data analysis carried out following the path loss measurements. Previous experiments for line-of-sight paths in the Arctic have shown that during the long winter night the atmosphere can be particularly stable from a propagation point of view. Since troposcatter radio transmissions rely on the continuous fluctuation of the random scatterers in the common volume, there was at the onset of this experiment, a concern that a stable troposphere, if present, might significantly increase the mean path loss value. This experiment shows that the tropospheric scatter conditions on this path were favorable to the scattering of the signal and remarkably invariant from month to month, even during the dark months November through March.

In summary, it has been found or confirmed that:

i) depending on the prediction method used, the measured long term median path loss value, L(50%), is 2.9 to 5.1 dB higher than the predicted values;

ii) there are no unusual effects on the long-term signal level statistics, during the long winter night;

iii) during these dark-winter months, the monthly median values were contained to within a range of about ±1 dB, which show that the tropospheric scatter conditions on this path are extremely stable[1];

iv) Monthly distributions of hourly median signal levels can be approximated by a normal law with standard deviations of about 1.0 dB;

v) the transmission is little affected by diurnal variations;

vi) short term signal level fluctuations appear to conform to a Rayleigh-type fading, especially during periods of slow fading[2];

vii) observed fade rates were typically of the order of 2.5, 7 and 18 fades or more per minute for percentages of time exceeding 90%, 50% and 10% respectively;

viii) periods of slow or fast fading could last a few hours to several days.

This experiment has demonstrated that, as far as propagation characteristics are concerned, and based on the present measurement set, a troposcatter link between Alert and Eureka is certainly feasible.

When CRC was first approached in 1988 to study the feasibility of a troposcatter system between Alert and Eureka, the requirements put forward by DND call for an operational system with relatively low transmission bit rate (a few hundreds kbps) capability. Since that time, the requirements have apparently been reassessed by DND and it is now understood that data rates of 4 to 6 Mbps will be needed.

The CRC experiment was not designed to determine the channel capabilities of the link but rather the long-term behavior of the propagation medium. The channel capacity was originally not an issue of concern and this aspect of the problem could only be addressed briefly in this report.

---

1. In the nondesert regions of the south, February is usually the worst month of the year for tropospheric transmissions [4].

2. The 10-90 percent fading range of the month of December 1992 is found to be 12.2 dB, which is somewhat smaller than expected for Rayleigh fading (13.4 dB). This suggests the presence of a small non-random signal component.

The High Arctic Troposcatter Experiment:
Final Report

C. Bilodeau and K. S. McCormick

1.0 INTRODUCTION

The most northerly settlement in Canada is Alert, being located at more than eighty-two degrees north latitude, and well below the horizon for communications with a geostationary satellite such as ANIK. At the present time, communications to the south are provided by a line-of-sight radio relay system that runs almost five hundred kilometres from Alert to the weather station Eureka at eighty degrees north latitude. From Eureka, an ANIK satellite is visible at near zero degrees elevation angle. Two earth stations are operated at Eureka in a vertical site diversity system to provide satellite communications to the south.

Since for large portions of the year the individual relay sites between the two settlements are inaccessible, it was decided to investigate the possibility of providing a tropospheric scatter link as a backup communications facility which could be used in the event of a failure of the radio relay system. Although standard prediction techniques indicated that such a link would probably be feasible, we were not able to find reference to troposcatter systems operating at such latitudes. An experiment was therefore planned to verify the propagation predictions. A site survey was carried out in the late summer of 1988, and two sites were selected - a transmitting site about one kilometre from an HF installation at Alert, and a receiving site on top of a hill about five kilometres from weather station Eureka. The distance between the two sites is 476 kilometres.

2.0 DESCRIPTION OF THE EXPERIMENT

The terrain between Alert and Eureka is quite mountainous, with the terrain often rising precipitously from sea level. At Eureka in particular, it was difficult to find a site in reasonable proximity to existing power lines, but with a small horizon angle in the direction of Alert. A site with reasonable access was finally chosen about five kilometres distant from the Eureka weather station and two kilometres distant from a power line. The coordinates of this location are 80°02'00"N latitude, and 86°13'00"W longitude. Its elevation is 314 m above mean sea level, the horizon angle to Alert was measured to be 5.8 milliradians. At Alert, because of electrical power constraints, a site was chosen at 82°27'00"N, 62°38'00"W. (Note that the lines of longitude are closely spaced at these latitudes). This location is on a broad plateau 194 m above mean sea level. Its horizon angle in the direction of Eureka is approximately 18 milliradians.

Major constraints on the design of the experiment were the relatively long path length and consequent large path loss, and the difficulty of the site access at Eureka. No heavy equipment would be available for the erection of the receiving antenna - its size had be to such that it could be erected manually by a small number of people. The compromises that were reached in the experiment design are described in the next section.
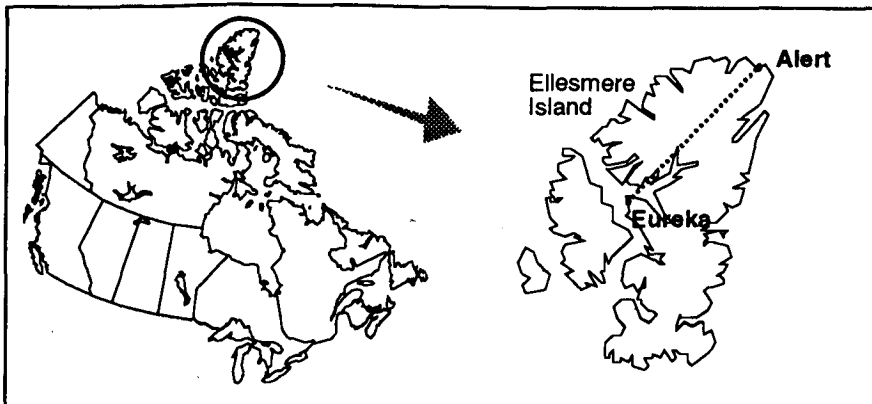

FIGURE 1.
Canada, with expanded view of the experimental region in the High Arctic. Alert is the most northerly settlement in Canada.
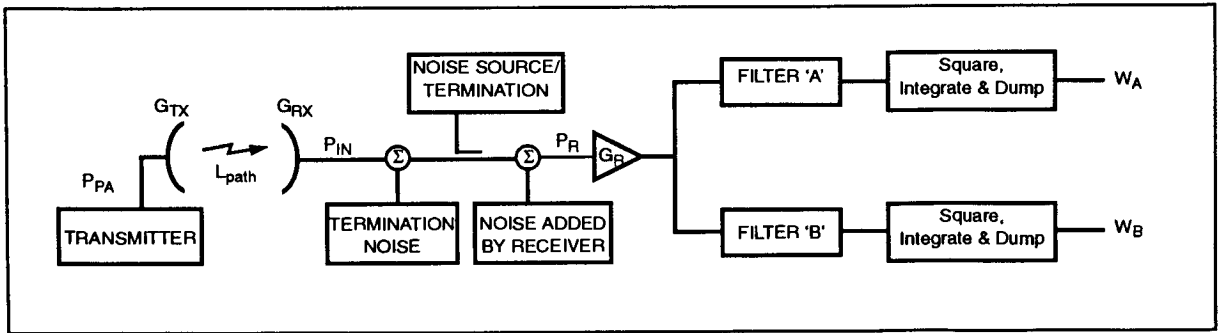
FIGURE 2. Simplified block diagram of troposcatter measurement system

3.0 THE MEASUREMENT SYSTEM

Because of their size and complexity, troposcatter communication systems are typically expensive. The measurement system that was designed for this experiment minimizes expenditure, installation and maintenance costs. A 4.5 metre dish antenna, consisting of a two-piece grid reflector, was selected as a trade-off between the desired physical and electrical characteristics. An antenna of larger dimension and weight would have provided more gain but could not have been installed easily by a crew composed of only 3 or 4 people or without access to some heavy motorized equipment. A frequency of 853 MHz was chosen as a compromise between reasonable antenna gain and path loss.

A custom tower was designed so that the antenna is attached to a 114 mm diameter pipe. The dish is installed so that the direction of the grids is vertical, defining the plane of polarization. This precaution did not prevent snow from accumulating at times between the reflector elements.

Because of the relatively low transmit power, a foam-filled coaxial feed could be used, eliminating the need for pressurization equipment.

The transmitter is designed to provide a transmission of constant UHF power of 100 W (+50 dBm). A dual channel power meter with full remote-control capability is attached to a directional coupler for sampling the forward and reflected power on the transmitter's low VSWR transmission line. An automated power measurement sub-system was programmed to maintain the power level at the transmitter antenna feed input to within ±2.3 W (±0.1 dB) of the nominal transmitted level. Losses from cables, couplers, sensor attenuators, etc., are all accounted for by the program. Power measurements, and corrections of the transmitted power level when required, are repeated four times per minute.

The antenna radiates a pure continuous wave (CW) produced by a low phase noise (< -82 dBcHz[-1] at 100 Hz offset from carrier) signal generator having an excellent long term frequency stability (aging rate better than 1 part in 10^8 per year).

Similarly, tight frequency tolerance is obtained at the receiver by phase-locking the receiver's local oscillators to a stable frequency standard. The use of a frequency standard at both the receive and transmit ends alleviates the need to perform frequent frequency-drift adjustments to accommodate a narrow receiver detection bandwidth of about 100 Hz.

The receiver must provide as much as 150 dB of signal amplification. Such a large overall amount of amplification is not easy to keep constant over wide temperature range or system life time. To minimize any amplification instability, the gain is distributed nearly evenly between the receiver's RF front end and two frequency down-conversion stages, one at 10 MHz, the other at 3 kHz. The first conversion provides good image rejection response whereas the second reduces the complexity of the analog-to-digital conversion circuitry. A special low noise amplifier (LNA) unit was designed and installed at the output of the receiving antenna feed. The components of the unit were mounted inside three miniature ovens to keep the operating temperature constant. In addition, a highly stable white noise source was coupled to the receiver signal main line to provide a reference power level for periodic (hourly) calibration of the LNA-receiver sub-system. The reference signal has less than 0.1 dB power variation over the temperature range of -50°C to +50°C and the unit introduces only 0.15 dB signal loss on the received signal path. The receiver has a noise figure of 0.90 dB.

The last stage of the receiver is implemented digitally after the signal has been digitized at a rate of about 10000 samples per second. It is composed of two narrow band pre-detection filters, a square-law detector, and a post detection integrate-and-dump circuit as explained later. The nominal signal frequency at the output of the 2nd IF stage is 2800 Hz.

Equipment at both the transmit and receive sites operate unattended. Eureka, the nearest settlement to the receive site, is five kilometres away and a line-of-sight UHF

telemetry link is used to relay the measurement data. Both sites are equipped with an uninterruptable power system able to sustain the equipment running for about 20 minutes during a main power line outage. The equipment is kept inside a 1.5 m × 3 m × 3 m shelter where the temperature is regulated.

4.0 DATA PROCESSING AND ACCURACY

In this section, an expression will be derived to relate the path loss (L_{path}) to the system parameters. A simplified model of the troposcatter measurement system is shown in Figure 2.

As mentioned in the previous section, the transmitting power is $P_{PA} = 100$ W. Each antenna provides 28.3 ±0.2 dBi gain ($G_{TX} = G_{RX}$) at 853 MHz, assuming a typical 50% antenna efficiency and a gain degradation factor of 0.9 dB.

Because of the high linearity of the system, the receiver can be modelled as a simple noiseless broadband RF amplifier preceded by a noise equivalent circuit to account for the thermodynamic degradation of the signal-to-noise ratio. The receiver has a gain G_r at the frequency of the carrier and the noise power added is determined from the receiver noise figure (NF= 0.90 dB).

The noise reference behaves like a simple passive 50 ohm termination when turned off.

Two more elements of the model shown in Figure 2 are the finite impulse response (FIR) bandpass filters which limit the detection bandwidth of the measurements following the digitization of the 2nd IF signal. Both filters are implemented using real-time digital signal processing technology. Filter A is centred around the incoming signal frequency whereas filter B is adjacent to it but still well within the passband of the 2nd IF stage. This second filter is required to reject the incoming signal during the calibration intervals.

Finally, the last elements in the model are the power detectors following the two bandpass filters. Detection is accomplished by squaring and integrating the incoming samples over a fixed interval of time.

An expression for determining the path loss is easily derived by relating the transmitter output power P_{PA} to the receiver input power P_{IN}:

$$L_{path} = \frac{P_{PA} G_{TX} G_{RX}}{P_{IN}} \qquad (1)$$

An expression is now needed to relate the receiver input power (P_{IN}) to its output (W_A). Two methods were used for determining the LNA-receiver sub-system power response. The first consisted of injecting a signal of known power and frequency, directly into the input of the unit. The detectors A and B output readings were

then recorded. Figure 3 shows the calibration curve obtained in this manner for the A detector when varying the input signal level in 0.1 dB increments.
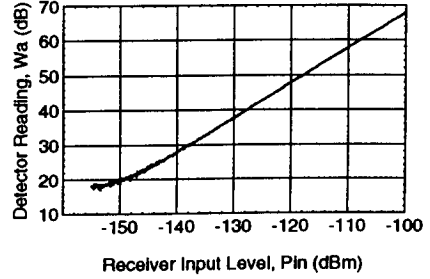

FIGURE 3. Power response for detector 'A'

The power response is linear for a carrier to noise ratio (C/N) greater than about 10 dB. At lower C/N, the response degrades gracefully as the thermal noise of the receiver predominates. This non-linearity can easily be removed by subtracting from it the average noise power as measured by detector B. The receiver response then becomes a straight line, having a slope of 1 and an intersect with the ordinate axis at $W_A = G_R$, so:

$$W'_A = P_{IN} + G_R \qquad (2)$$

where G_R is the receiver gain expressed in dB and W'_A is the detector reading corrected for low C/N ratios.

The second method used for calibrating the LNA-receiver sub-system is a spot measurement of the readings obtained at the detectors output A and B when the noise source is turned 'ON'. Knowing the excess noise ratio (ENR) of the reference noise source and the equivalent noise bandwidth (ENB) of the detection filters, the reference noise power (RNP) can be found as follows:

$$RNP = 10 \log (kT \, ENB) + ENR \qquad (3)$$

where:

k is Boltzmann's constant (1.38×10^{-20} mJK^{-1}),
T is the standard temperature (290K).

The ENR was measured to be 26.6 dB using a calibrated ENR meter. The ENB can be determined from the following equation:

$$ENB = \frac{\int_{-\infty}^{\infty} |H(\omega)|^2 d\omega}{|H(\omega_0)|^2} \qquad (4)$$

3

where $|H(\omega)|$ is the magnitude of the frequency response of the detection filter and $\omega_0/2\pi$ is its centre frequency. For an FIR type of filter, $H(\omega)$ is given by:

$$H(\omega) = \sum_{k=0}^{M-1} b_k e^{-j\omega k} \qquad (5)$$

where the filter coefficients $\{b_k\}$ are the values of the unit sample response of the filter and M is the filter length. Equations 4 and 5 were evaluated numerically over the frequency range of interest for filters A (M_A = 163 coefficients) and B (M_B = 82 coefficients) used in the experiment. Table 1 summarizes the results.

Table 1: Comparison of reference levels using the two calibration methods.

FILTER	ENB	Method 1 P_{in}	Method 2 RNP	Δ P_{in} - RNP
	(Hz)	(dBm)	(dBm)	(dB)
A	140.6	-126.0	-125.9	-0.1
B	146.7	-125.7	-125.7	0.0

The third column of the table shows the signal level injected at the LNA unit input when applying the first method to achieve the same detector output readings as recorded for method 2. The results of both methods agree within 0.1 dB.

5.0 DATA ANALYSIS

Early in the design of the experiment, because of the remoteness of the location, it was recognized that the data collection for the experiment would have to be severely restricted. Personnel at the Eureka Weather Station agreed to look after the data recording computer, but the large number of signal measurements made (20 per second on each of the two signal channels) would have placed an impossible burden on them. Even with an effective data compaction scheme, the data storage requirements would have exceeded 300 kilobytes per hour.

Accordingly, it was decided to carry out as much preprocessing as possible at the recording site, and to retain only essential information on a routine basis. The data at the receiver were packetized, sent by telemetry to the weather station, and each hour the signal level density distribution for that hour, the median signal levels for each minute, each five minutes and the hour, the average power levels in both the signal and noise channels, a five-second sample of the actual data, and some housekeeping data were recorded. This scheme allowed the use of a single floppy disk each month, which was mailed to the laboratory in Ottawa.

For a few months, it was possible to transmit the original packetized data to Ottawa over a satellite link, in order to record samples of the details of the signal level characteristics.

In an experiment such as this, in which large volumes of data are recorded from a remote location, it is a significant problem to ensure that the data are valid: i.e. that there are no undetected periods in which either the transmitter/receiver/recording chain was faulty, or in which external factors affected the received signal. Since the original data were not generally available, a number of tests were applied to the data and these were plotted in a form that was easily scanned visually to detect anomalies. The following plots were generated for each day's data: the signal level density distribution and the cumulative signal level distribution for each hour, a time series of the median signal level distributions for each minute of the day, a time series of the hourly median signal level, noise level, and injected calibration power, the measured frequency offset between the transmitter and receiver and the twenty-four five-second samples of the receiver signal. As a final check, the difference between the ten percent and ninety percent levels of the cumulative signal distributed were calculated and plotted. (For a Rayleigh distribution, this value is expected to be 13.4 dB.) All these plots were put on a single letter-size page for each day, permitting a rapid visual scan of the data characteristics.

5.1 Signal Level Characteristics

The signal level characteristics are discussed under four headings:

> Fading rate
> Short term signal level fluctuations
> Long term signal level fluctuations
> Predictions

Fading Rate

The received signal level exhibited periods of both rapid and slow fading. Using data from the period for which all the packetized data were recorded, Figures 4 and 5 show typical examples of both these conditions. In each case, the horizontal line shows the median signal level calculated for a one-hour period. The signal levels typically rise above the median by more than 5 dB, and fall by more than 20 dB into the system noise.

One of the quantities of interest to the system designer is the "fade rate", defined as the number of two-way median crossings in a given time interval such as one minute or one hour. It was possible to calculate a number of these fade rates from the detailed signal level time series that were received in Ottawa, and the results are shown in Figure 6. In performing the calculation, a "hysteresis" zone was set up around the median to eliminate small fluctuations from affecting the results. In other words, a median crossing was not counted unless the signal continued its path sufficiently to exit the "hysteresis" zone. The fade rates were calculated for
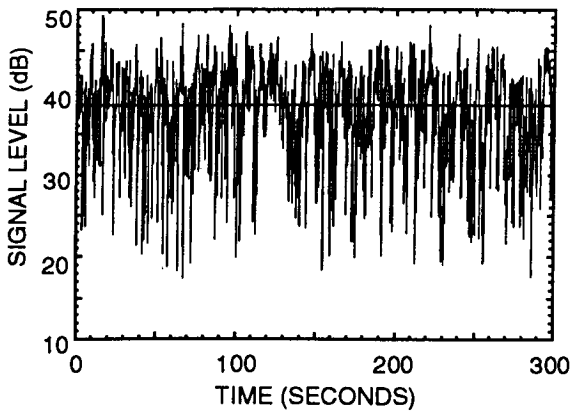
4

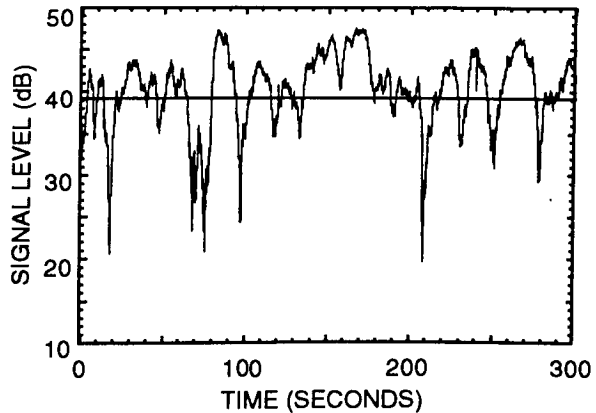FIGURE 4. Example showing typical received signal level variations during a period of fast fading

FIGURE 5. Example showing typical received signal level variations during a period of slow fading
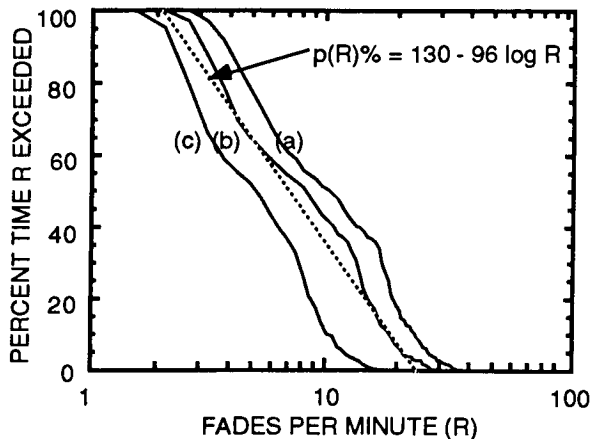

$p(R)\% = 130 - 96 \log R$

FIGURE 6. Fade rate distributions for the month of April 1992 with "hysteresis": (a) ±1 dB, (b) +1/-3 dB, (c) +1/-10 dB (see text)
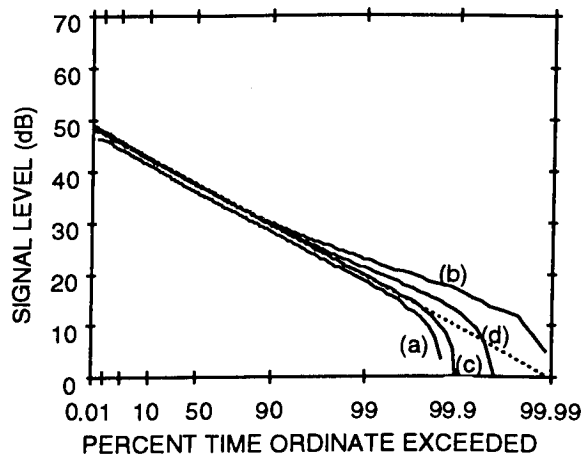

FIGURE 7. Cumulative distributions of data recorded during December 1992 for periods of one hour, (a) slow fading, (b) fast fading; and periods of several days (c) slow fading, (d) fast fading
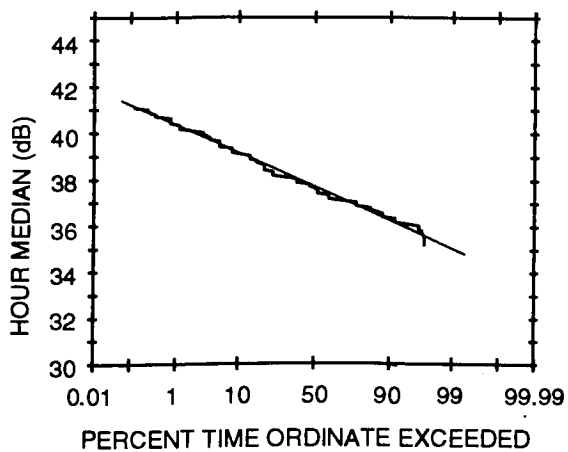

FIGURE 8. Cumulative distribution of hourly median signal levels for the month of December 1991
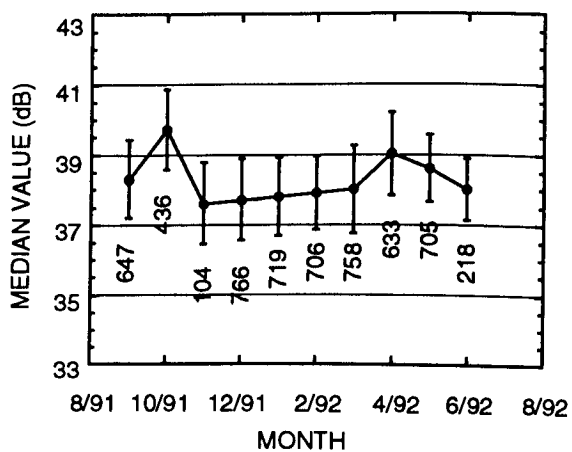

FIGURE 9. Monthly median values of the cumulative distributions of hourly median signal levels. The error bars indicate one standard deviation and each number, the available number of hour medians

5

different values of the hysteresis zone, including one dB above the median to one dB below it, one dB above to three dB below, and one dB above to ten dB below. The results are shown in the Figure. Curves (a), (b), and (c) were calculated for all the available data for the month of April 1992, 398 hours. For the larger hysteresis zones, the number of fades included in the calculation decreases. There is perhaps a tendency for the higher fade rates to decrease more than the lower ones, but the change in slope of the curves is not large. The dashed line on the plot represents a linear fit to the (+1, -3) case.

Short Term Signal Level Fluctuations

Figure 7 shows a series of cumulative probability distributions calculated for data recorded during December 1992. Curves (a) and (b) show distributions calculated for one hour periods in slow and fast fading conditions, respectively. During slow fading, curve (a) appears to conform very well to a Rayleigh-type fading, as evidenced by the straight line characteristic extending from 0.01 percent to more than 99 percent of the hour, whereas curve (b) for the fast fading period departs from the straight line for percentages in excess of ninety percent. Similar behaviour is found for curves (c) and (d) which encompass data from complete days of slow and fast fading. Interestingly, when the distribution is calculated for the whole month, it is found to be essentially identical to curve (c). The 10-90 percent fading range in this case is found to be 12.2 dB, which is somewhat smaller than expected for Rayleigh fading (13.4 dB).

Long Term Signal Level Fluctuations

The primary purpose of this experiment was to gain a knowledge of the long-term signal level statistics. In this case it is the monthly signal level median values that are of interest. For each month, a distribution was formed of all the hourly median signal levels for that month. An example for December 1991 is shown in Figure 8. Here the data are plotted on a Gaussian axis, and as expected the plot indicates that the medians follow a normal distribution. In this case, the monthly median value of the hourly medians is 37.7 dB, with a standard deviation of 1.1 dB. Figure 9 shows the monthly median values of the hourly medians for all the available data. In this plot, the numbers on the error bars indicate the number of hour medians that were used to form the corresponding distribution. The reason that in some cases they exceed the number of hours in the month is due to an artifact in the data recording setup. Sometimes the recording for a month extended a day or two into the following month. Figure 9 is remarkable in that it shows that the tropospheric scatter conditions on this path were extremely stable during the measurement period, particularly during the dark months November through March. During the total observation period, these median

values were contained to within about ±1 dB, with standard deviations of about 1 dB.

The next section will assume that a scale reading of 38 dB can be used to represent the long-term median for 50 percent of the time. Using the calibration curve of Figure 3, this value translates into a long-term received power of -129.5 dBm. Assuming a transmitter power of 100W, a total gain degradation factor of 1.8 dB for the two antennas, and equal receive and transmit antenna gains of 29.2 dB, we find a long-term path loss of 236.3 dB.

Predictions

Three different methods were used to predict the long-term median path loss L(50%). The first was through an in-house propagation prediction program, using a method based on NBS Tech. Note 101. The other two were CCIR methods as given by Roda [4]. Where necessary a continental temperate climate was assumed since no information is available for a polar climate. These predictions yielded 231.2, 232.7, and 233.4 dB. In these calculations, the take-off angle for the transmitter is somewhat uncertain. It was assumed to be 18 milliradians, a value which was measured during the initial site survey, but which was unfortunately not verified during the actual antenna installation. (The sensitivity of the prediction to errors in take-off angle is about 0.3 dB per milliradian). The difference between the measured long-term median and the predicted values varies from 2.9 to 5.1 dB. Given the uncertainties in some of the experimental parameters as well as the prediction techniques, this agreement is considered acceptable.

6.0 SYSTEM FEASIBILITY

Previous experience has shown that during the long winter night the cold, dry arctic atmosphere can be particularly stable from a propagation point of view, presumably because of the absence of diurnal solar heating and cooling. Since troposcatter radio transmissions rely on the continuous fluctuation of the random scatterers in the common volume, there was at the onset of this experiment a concern that a stable troposphere, if present, might significantly increase the mean path loss value or exhibit unusual effects. This experiment shows that the tropospheric scatter conditions on this path were favorable to the scattering of the signal and remarkably invariant from month to month, even during the dark months November through March.

This experiment has demonstrated that, as far as propagation characteristics are concerned, and based on the present measurement set, a troposcatter link between Alert and Eureka is certainly feasible.

When CRC was first approached in 1988 to study the feasibility of a troposcatter system between Alert and Eureka, the requirements put forward by DND called for
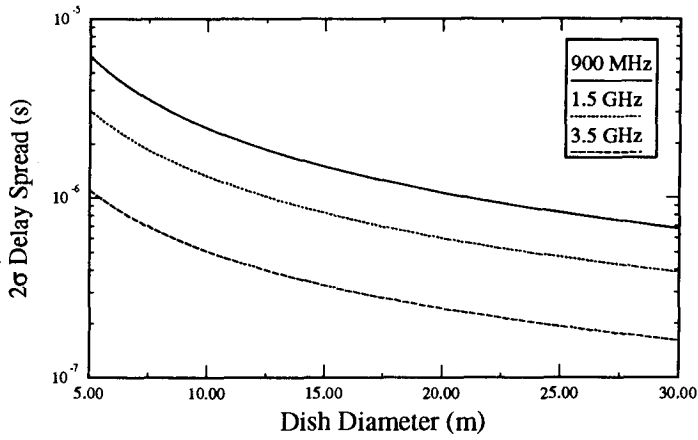
FIGURE 10. Estimate of multipath delay spread using Sunde model
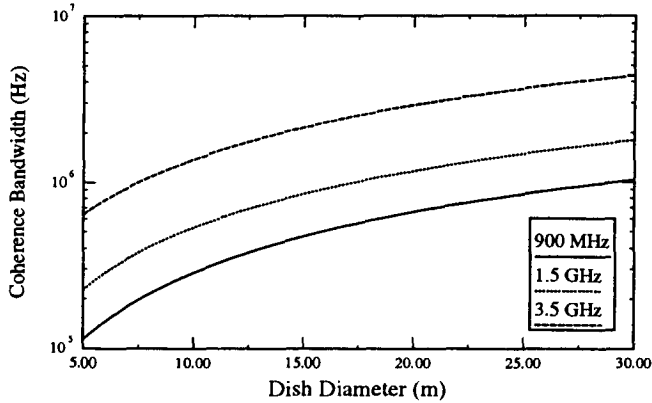for various carrier frequency and parabolic dishes diameter

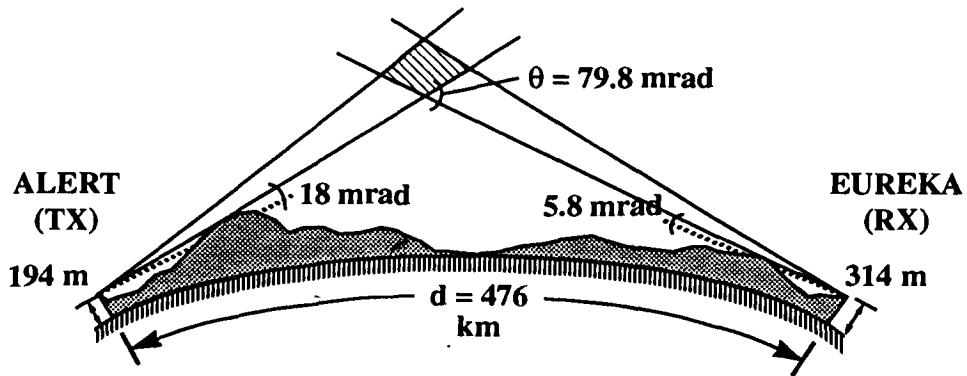FIGURE 11. Coherence bandwidth derived from delay spreads of Figure 10 above.

FIGURE 12. Path geometry of the link Alert-Eureka as used in the Sunde model.

7

an operational system with relatively low transmission bit rate (a few hundreds kbps) capability. Since that time, the requirements have apparently been reassessed by DND and it is now understood that data rates of 4 to 6 Mbps will be needed.

The CRC experiment was not designed to determine the channel capabilities of the link but rather the long-term behavior of the propagation medium. The channel capacity was not originally an issue of concern and remains a matter that is outside the scope of this study. Nevertheless, the following discussion is offered.

For practical purposes, the transmission capabilities of the short-term time-varying channel can be characterized in terms of its spread and bandwidth parameters.

The experiment shows that the frequency of occurence of the fades is mostly contained within the range .04-0.3 fades per second. This gives an indication of the width of the Doppler spectrum or the Doppler spread B of the signal, roughly:

$$(0.04 \le B \le 0.30) \, \text{Hz} \tag{6}$$

Obviously, the scatterers move slowly when compared to the frequencies to be contained in the high data rate troposcatter signal. The Doppler spread will therefore have a minimal effect on the bandwidth of the system. However, if we assume that the channel time-correlation is given by $T = 1/B$ then we can expect to see statistically correlated signal samples for a minimum time $t \ll 3.3$ s when substituting the worst case value $B = 0.30$ given in (1). During this minimum correlation time of $t \ll 3.3$ s we can assume the channel to be quasi-stationnary. This time can be used to acquire information on the state of the channel before it changes, and this is exploited in diversity techniques.

Next is the question of spectrum distortion due to the multipath delay spread. There is no known reliable method for predicting the multipath delay spectrum. The Bello model, the Rice model or the Sunde model are among the current methods used today and give only an approximate evaluation of the multipath delay spread. The latter method was used to calculate the multipath delay spread shown in Figure 10, as given in [4] by:

$$L = 2\sigma = \frac{d}{2c} (\omega^2 + \omega\theta) \tag{7}$$

where σ is the r.m.s. duration of the received impulse, d is the path length (km), c is the velocity of light (km-s^{-1}), ω is the path beamwidth (in radians) of the antennas and θ is the scattering angle in radians. The calculation assumes that the illumination efficiency of the antennas is 70% of the theoritical 3 dB beamwidth (ω_{3dB}) of the parabolic antennas; that is,

$$\omega = \omega_{3dB} \times 70\% = \frac{21000}{fD} \times 0.7 \tag{8}$$

where f is the signal frequency (MHz) and D is the antenna diameter (m). From equation 7, the coherence bandwidth can be derived as:

$$W = \frac{0.7}{L} = \frac{1.4c}{d(\omega^2 + \omega\theta)} \tag{9}$$

Curves calculated using this last expression are shown in Figure 11. The path geometry shown in Figure 12 applies to both Figures 10 and 11.

Despite the semi-emperical nature of the Sunde model, it is probably safe to conclude from these figures that transmission rates in excess of about 1 Mbps would most likely require the use of high modulation level, adaptive channel equalization, large dish diameter and/or higher frequency transmission. Also, for transmission rates of 4-6 Mbps, multiple channels (systems) would be required if the carrier frequency is to remain around 900 MHz.

8.0 REFERENCES

[1] 2790-1 (DCEM-s) 27 May 1988 (NOTEL)

[2] *"Climatological Report"*, Project P-8126, Harris Corp., Rochester, N.Y., April 1988

[3] *"Alert to Eureka Troposcatter System - Site Survey Report"*, Project P-8126, Harris Corp., Rochester, N.Y., September 1988

[4] G. Roda, *"Troposcatter Radio Links"*, Artech House Inc., 1988, ISBN 0-89006-293-5

[5] C. Bilodeau and K.S. McCormick, *"Propagation Measurements on a Troposcatter Link in the Canadian High Arctic"*, in AGARD Conference Proceedings of the 53rd Symposium of the Electromagnetic Wave Propagation Panel, Rotterdam, 4-8 October 1993 (to be published).

SECURITY CLASSIFICATION OF FORM
(highest classification of Title, Abstract, Keywords)

DOCUMENT CONTROL DATA

(Security classification of title, body of abstract and indexing annotation must be entered when the overall document is classified)

1. ORIGINATOR (the name and address of the organization preparing the document. Organizations for whom the document was prepared, e.g. Establishment sponsoring a contractor's report, or tasking agency, are entered in section 8.) COMMUNICATIONS RESEARCH CENTRE P.O. BOX 11490, STATION H 3701 CARLING AVENUE OTTAWA, ONTARIO K2H 8S2	2. SECURITY CLASSIFICATION (overall security classification of the document. including special warning terms if applicable) UNCLASSIFIED

3. TITLE (the complete document title as indicated on the title page. Its classification should be indicated by the appropriate abbreviation (S,C or U) in parentheses after the title.)

HIGH ARCTIC TROPOSCATTER EXPERIMENT - FINAL REPORT (U)

4. AUTHORS (Last name, first name, middle initial)

BILODEAU, C., AND MCCORMICK, K.S.

5. DATE OF PUBLICATION (month and year of publication of document) APRIL 1994	6a. NO. OF PAGES (total containing information. Include Annexes, Appendices, etc.) 11	6b. NO. OF REFS (total cited in document)

7. DESCRIPTIVE NOTES (the category of the document, e.g. technical report, technical note or memorandum. If appropriate, enter the type of report, e.g. interim, progress, summary, annual or final. Give the inclusive dates when a specific reporting period is covered.)

FINAL REPORT

8. SPONSORING ACTIVITY (the name of the department project office or laboratory sponsoring the research and development. Include the address.) DCEM
DEFENCE RESEARCH ESTABLISHMENT OTTAWA
SHIRLEYS' BAY
OTTAWA, ONTARIO K1A 0Z4

9a. PROJECT OR GRANT NO. (if appropriate, the applicable research and development project or grant number under which the document was written. Please specify whether project or grant) 041WE	9b. CONTRACT NO. (if appropriate, the applicable number under which the document was written)
10a. ORIGINATOR'S DOCUMENT NUMBER (the official document number by which the document is identified by the originating activity. This number must be unique to this document.) CRC-RP-94-002	10b. OTHER DOCUMENT NOS. (Any other numbers which may be assigned this document either by the originator or by the sponsor)

11. DOCUMENT AVAILABILITY (any limitations on further dissemination of the document, other than those imposed by security classification)

(X) Unlimited distribution
( ) Distribution limited to defence departments and defence contractors; further distribution only as approved
( ) Distribution limited to defence departments and Canadian defence contractors; further distribution only as approved
( ) Distribution limited to government departments and agencies; further distribution only as approved
( ) Distribution limited to defence departments; further distribution only as approved
( ) Other (please specify):

12. DOCUMENT ANNOUNCEMENT (any limitation to the bibliographic announcement of this document. This will normally correspond to the Document Availabilty (11). However, where further distribution (beyond the audience specified in 11) is possible, a wider announcement audience may be selected.)

13. ABSTRACT (a brief and factual summary of the document. It may also appear elsewhere in the body of the document itself. It is highly
desirable that the abstract of classified documents be unclassified. Each paragraph of the abstract shall begin with an indication of the
security classification of the information in the paragraph (unless the document itself is unclassified) represented as (S), (C), or (U).
It is not necessary to include here abstracts in both offical languages unless the text is bilingual).

Experimental results of radio propagation measurements at 853 MHz are given for
a 500 km troposcatter link in the Canadian High Arctic. Statistical analysis
of path loss and fading measurements are presented.

The experimental data were acquired using a narrowband measurement system that was
developed to permit a transmitting power of only 100 Watts while using a 4.5
meter dish at each end of the link. The system includes a digital signal processor
(DSP) receiver for signal strength computation and a high stability noise source
reference for amplitude calibration. The main characteristics of this system are
described in this paper.

Detailed fading distributions are presented for examples of slow and fast fading
periods and compared with Rayleigh distributions. An estimate of the long term
median path loss is made and compared with values predicted using accepted
techniques. The results are believed to be the first ever presented for a
microwave troposcatter link above the 80th parallel.

14. KEYWORDS, DESCRIPTORS or IDENTIFIERS (technically meaningful terms or short phrases that characterize a document and could be
helpful in cataloguing the document. They should be selected so that no security classification is required. Identifiers, such as equipment
model designation, trade name, military project code name, geographic location may also be included. If possible keywords should be selected
from a published thesaurus. e.g. Thesaurus of Engineering and Scientific Terms (TEST) and that thesaurus-identified. If it is not possible to
select indexing terms which are Unclassified, the classification of each should be indicated as with the title.)